Voltage-dependent Na^+ channel phenotype changes in myoblasts. Consequences for cardiac repair

Ramón Martínez-Mármol [a,b], Miren David [e], Rosario Sanches [b], Meritxell Roura-Ferrer [a,b], Núria Villalonga [a,b], Eleonora Sorianello [b,c], Susan M. Webb [d], Antonio Zorzano [b,c], Anna Gumà [b], Carmen Valenzuela [e], Antonio Felipe [a,b,*]

[a] *Molecular Physiology Laboratory, Universitat de Barcelona, Spain*
[b] *Departament de Bioquímica i Biología Molecular, Universitat de Barcelona, Spain*
[c] *Parc Cientific de Barcelona, Universitat de Barcelona, Spain*
[d] *Departament de Endocrinologia i Medicina, Hospital Sant Pau, Universitat Autonoma de Barcelona, Spain*
[e] *Instituto de Farmacología y Toxicología, CSIC/UCM, Universidad Complutense de Madrid, Spain*

Abstract

Objective: Cellular cardiomyoplasty using skeletal myoblasts is a promising therapy for myocardial infarct repair. Once transplanted, myoblasts grow, differentiate and adapt their electrophysiological properties towards more cardiac-like phenotypes. Voltage-dependent Na^+ channels (Na_v) are the main proteins involved in the propagation of the cardiac action potential, and their phenotype affects cardiac performance. Therefore, we examined the expression of Na_v during proliferation and differentiation in skeletal myocytes.

Methods and results: We used the rat neonatal skeletal myocyte cell line L6E9. Proliferation of L6E9 cells induced $Na_v1.4$ and $Na_v1.5$, although neither protein has an apparent role in cell growth. During myogenesis, $Na_v1.5$ was largely induced. Electrophysiological and pharmacological properties, as well as mRNA expression, indicate that cardiac-type $Na_v1.5$ accounts for almost 90% of the Na^+ current in myotubes. Unlike in proliferation, this protein plays a pivotal role in myogenesis. The adoption of a cardiac-like phenotype is further supported by the increase in $Na_v1.5$ colocalization in caveolae. Finally, we demonstrate that the treatment of myoblasts with neuregulin further increased $Na_v1.5$ in skeletal myocytes.

Conclusion: Our results indicate that skeletal myotubes adopt a cardiac-like phenotype in cell culture conditions and that the expression of $Na_v1.5$ acts as an underlying molecular mechanism.

Keywords: Sodium channels; Cardiomyoplasty; Myogenesis; Skeletal myoblast; Cardiac repair

1. Introduction

Cellular therapy is a promising strategy for heart failure [1–3]. Following myocardial infarction, the muscle becomes a non-contractile fibrous scar. Myocardium cannot fully regenerate because cardiac muscle cells do not re-enter the cell cycle. Unlike cardiomyocytes, skeletal myocytes proliferate and differentiate, thereby generating electrically excitable fibres [3]. Skeletal myoblasts, cardiomyocytes, and bone

AF designed research. AZ coordinated human biopsies and contributed with reagents. SMW collected human samples. ES isolated human myoblasts. RMM, MD and CV performed electrophysiology. RMM, RS, MRF, NV undertook research. RS and AG performed NRG experiments. RMM, MD, CV and AF analysed data. AF and CV wrote the paper.

* Correspondence author. Molecular Physiology Laboratory, Departament de Bioquímica i Biología Molecular, Universitat de Barcelona, Avda Diagonal 645, E-08028 Barcelona, Spain. Tel.: +34 934034616; fax: +34 934021559.

E-mail address: afelipe@ub.edu (A. Felipe).

marrow mononuclear cells have been transplanted to replace lost myocardial tissue [1–4]. Autologous transplantation into the infarcted myocardium improves myocardial performance both in vitro and in vivo [1–3]. However, the mechanisms underlying improved cardiac function remain uncertain.

Muscle excitability is generated by the incorporation of ion channels into the surface membrane [5]. Voltage-dependent sodium channels (Na_v) are the main proteins involved in propagating action potential in nerve and muscle [6,7]. Na_v gene family comprises different members ($Na_v1.1$–$Na_v1.9$, Na_vX), and based on their sensitivity to tetrodotoxin (TTX), they are separated into TTX-sensitive and TTX-resistant [6,8]. Cardiac and skeletal muscles express different genes. While adult skeletal muscle expresses predominantly a TTX-sensitive channel ($Na_v1.4$), adult cardiomyocytes mostly present a TTX-resistant protein ($Na_v1.5$) [9,10]. However, development and muscle denervation regulate their expression [5,11–13]. For instance, TTX-sensitive currents increase and TTX-resistant channels decrease with age in skeletal muscle, but denervation counteract this phenotype [5,12,13]. $Na_v1.5$ accounts for ~90% of the Na^+ currents in the adult mammalian heart, thus determining major electrophysiological and pharmacological properties. The relative participation of other isoforms is uncertain [5,11].

The success of cellular cardiomyoplasty based on skeletal myocytes would be strongly dependent upon the acquisition of the Na_v cardiac-like phenotype. The ability of skeletal myoblast to myoregenerate, as well as their resistance to ischemia, allows these cells to grow quickly within the infarcted area and generate myofibers [1–4]. Pre-treating myoblasts before transplantation has been proposed to increase cardiac-like properties [14,15]. By using neonatal-derived skeletal myoblasts, we demonstrate that myotubes improve the Na_v cardiac-like phenotype *in vitro*. Since myoblast proliferation and differentiation are important in graft generation, we characterized Na_v expression in skeletal myoblasts in culture. Proliferation increased $Na_v1.4$ and $Na_v1.5$ expression. However, neither protein has an apparent role in the cell cycle progression. Myotube differentiation induces $Na_v1.5$, which triggers a cardiac-like phenotype. $Na_v1.5$ plays a pivotal role in myogenesis. Furthermore, neuregulin-1, a growth factor that regulates differentiation and which has been implicated in the protection and survival of cardiac and skeletal muscle, further increased the adoption of a cardiac-like Na_v phenotype. Our results suggest that myoblasts originating from an early state of differentiation and treated in culture prior to transplantation, adopt more optimal electrical cardiac phenotypes.

2. Methods

2.1. Cell culture

The rat skeletal muscle-derived L6E9 cell line was kindly provided by Dr. B. Nadal-Ginard (Cardiovascular Institute and Center for Cardiovascular Health, Mount Sinai School of Medicine, NY). Myoblasts were grown in Dulbecco's modified medium (DMEM) supplemented with 10% fetal bovine serum (FBS), antibiotics, 2 mM L-glutamine, and 25 mM Hepes (pH7.4). Pre-confluent myoblasts (70–80%) were induced to differentiate by lowering FBS to a final concentration of 2%. In some experiments, aqueous solutions of TTX (Alomone) were simultaneously added to the media. Recombinant neuregulin 1 containing the bioactive EGF domain, heregulin-β_1 (NRG), was from PromoKine.

Primary culture of adult human skeletal muscle myoblasts were obtained from a deltoid muscle biopsy. The sample was minced and cultured as previously described [16]. Myoblast were cultured in 75% DMEM and 25% M199 medium, supplemented with 10% FBS, 2 mM glutamine, antibiotics, 0.25 μg/ml fungizone, 10 μg/ml insulin, 10 ng/ml epidermal growth factor, and 25 ng/ml fibroblast growth factor. To obtain highly purified myoblasts, primary cultures were sorted for the early surface marker CD56 by immunomagnetic selection [16]. CD56-positive cells were seeded in the medium containing 15% FBS until ~80% confluence. Myogenesis was induced by lowering FBS to 2%.

2.2. Proliferation assay

DNA synthesis was determined by the incorporation of ^{3}H-thymidine (GE Healthcare) into DNA. L6E9 cells (2×10^4) were seeded in 24-well plates without FBS, supplemented with 0.2% BSA, for 36 h. Cells were further cultured for 24 h in the absence (resting) or presence (proliferation) of 10% FBS with/without aqueous solutions of TTX. Finally, this was replaced by the same medium containing 1 μCi/ml [^{3}H]-thymidine. After three hours, cells were fixed in 70% methanol, washed three times in ice-cold 10% trichloracetic acid, and solubilized in 1% SDS and 0.3% NaOH. The content of the well was used for counting radioactivity.

2.3. RNA isolation, RT-PCR analysis and real-time PCR

Total RNA from rat tissues (brain, heart, and skeletal muscle) and L6E9 cells was isolated using the Tripure reagent (Roche Diagnostics). All aspects of this investigation conformed to the *Guide for the Care and Use of Laboratory Animals* published by the US National Institutes of Health (NIH Publication No. 85-23, revised 1996). RNA was treated with DNaseI and PCR controls were performed in the absence of reverse transcriptase. cDNA synthesis was performed with transcriptor reverse transcriptase (Roche) with a random hexanucleotide and oligo dT, according to the manufacturer's instructions. Once cDNA was synthesized, the conditions were set for further PCR: 94 °C for 1 min, 1 min at the corresponding annealing temperature (see Table 1 in Supplementary Material (SM)), and 72 °C for 1 min. These settings were applied for 30 cycles.

Real-time PCR was performed using a LightCycler machine with LightCycler FastStart DNA Master^{PLUS} SYBR Green I (Roche). The reactions for $Na_v1.4$ and $Na_v1.5$ (specific $Na_v1.5$ settings in parenthesis) were performed as follows: 95 °C for 5 s, 61 °C (58 °C) for 6 s, 72 °C for 9 s (11 s) and 85 °C for 2 s,

preceded by 10 min at 95 °C and followed by 10 s at 95 °C and 30 s at 65 °C. 18 S was included as an internal reference. The chosen forward and reverse PCR primers, PCR annealing temperatures, PCR product length and accession numbers are shown in SM Table 1. The real-time PCR efficiency (E) of one cycle in the exponential phase was calculated according to the equation: $E = 10^{(-1/\text{slope})}$. The normalized $Na_v1.5/Na_v1.4$ ratio was calculated as follows: Ratio $= (1+E)^{\Delta Ct\ (Na_v1.5)} / (1+E)^{\Delta Ct\ (Na_v1.4)}$, where Ct signifies the threshold cycle.

2.4. Membrane protein extracts and Western blot

Cells were washed in cold phosphate-buffered saline (PBS) and lysed on ice with lysis solution (1% NP40, 10% glycerol, 50 mmol/L HEPES pH 7.5, 150 mmol/L NaCl), supplemented with 1 μg/ml aprotinin, 1 μg/ml leupeptin, 86 μg/ml iodoacetamide and 1 mM phenylmethylsulfonyl fluoride as protease inhibitors. To obtain enriched membrane preparations, homogenates were centrifuged at 3000 *g* for 10 min and the supernatant was further centrifuged at ~150,000 *g* for 90 min. The pellet was resuspended in 30 mM HEPES (pH 7.4). To concentrate enriched membrane proteins from L6E9 cells, Microcon centrifugal filter devices (Amicon) were used.

Crude membrane protein samples were separated on 7.5% SDS-PAGE, transferred to nitrocellulose membranes (Immobilon-P, Millipore) and blocked in 5% dry milk-supplemented 0.2% Tween 20 PBS. Filters were immunoblotted with antibodies against $Na_v1.5$ (1/200, Alomone), myosin heavy chain (MHC; 1/20, MF20-anti-meromyosin — from Developmental Studies Hybridoma Bank), myogenin (1/20, F5D, DSHB), Na/K ATPase α_1-subunit (1/100, α6F, DSHB), caveolin 3 (1/5000, BD Biosciences) and pan-caveolin (1/200, BD Biosciences). As a loading and transfer control, we used a monoclonal anti-β-actin antibody (1/5000, Sigma).

2.5. Immunolocalization, nuclei staining and fusion index

A Monoclonal Anti-pan-Sodium Channel (1/100, clone K58/35, Sigma) was used. Anti-caveolin polyclonal (1/250), which recognizes caveolin isoforms 1, 2, and 3, was from BD Biosciences. CY2 and CY3 secondary antibodies (1/250) were from Amershan.

L6E9 cells fixed with 4% paraformaldehyde in PBS for 10 min were further permeabilized with 1% Triton X-100/PBS for 10 min. After 60 min incubation with blocking solution (10% goat serum/5% non fat dry milk/0.75% Triton X-100/PBS), cells were reacted with antibodies in 10% goat serum/0.75% Triton X-100/PBS for 90 min. Cells were further incubated with CY3 anti-rabbit antibody in PBS. CY2 anti-mouse was used for caveolin visualization. For nuclei staining, fixed and permeabilized cells were stained with DAPI (50 ng/ml) in PBS for 2 min. Under a fluorescent microscope, several randomly chosen fields were photographed, and the nuclei per cell were counted. The fusion index was calculated as follows: Fusion Index (%) = (number of nuclei in myotubes / total number of nuclei in the field) * 100.

2.6. Electrophysiology

L6E9 cells were held at −120 mV and Na^+ currents generated by 10 ms square pulses from −90 mV to +60 mV in 10 mV steps. Normalized conductance was set by using Boltzmann's equation: $G/G_{max} = 1/(1+\exp((V_{1/2}-V)/k))$. V_h is the voltage at which the current is half activated and k is the slope factor of the activation curve. To calculate voltage-dependent inactivation, cells were held at −120 mV and pre-pulses (2.75 s) to various potentials, ranging from −140 mV to +10 mV in 10 mV steps, followed by a test pulse of −10 mV during 80 ms were applied. Steady-state inactivation plots were fitted to a Boltzmann equation: $I/I_{max} = 1/(1\text{-}\exp((V_{1/2}-V)/k))$. Currents were recorded at room temperature (21–23 °C) using the whole cell patch-clamp technique with an Axopatch 1C amplifier (Axon Instruments). Micropipettes were pulled from borosilicate glass capillary tubes (GD-1; Narishige) using a P-87 puller (Sutter Instrument). The intracellular pipette solution contained (in mM) 5 NaCl, 5 KCl, 130 CsF, 1 $MgCl_2$, 4 MgATP, 10 HEPES-K, and 5 EGTA and adjusted to pH 7.2 with CsOH. The bath solution contained (in mM) 140 NaCl, 5 KCl, 1.8 $CaCl_2$, 1 $MgCl_2$, 10 HEPES-Na, 10 glucose, 20 TEA, and 2 $CoCl_2$ and adjusted to pH 7.4 with NaOH. TTX (Alomone) was dissolved in water. Micropipette resistance was set at 1–2 MΩ. Data analysis was performed using pClamp 9.0.1 and Origin 7.0.3 (Microcal Software).

Fig. 1. L6E9 myoblasts express voltage-dependent Na^+ channels. (A) Representative traces of Na^+ currents. Cells were held at −120 mV and pulse potentials were applied. (B) Current intensity as a function of membrane potential. L6E9 cells were held at −120 mV and currents were evoked by 10 ms square pulses from −90 mV to +60 mV in 10 mV steps. (C) Normalized conductance (●) and Steady-state availability (○) curves plotted against test potentials. To calculate steady-state inactivation cells were held at −120 mV and pre-pulses (2.75 s) to various potentials, ranging from −140 mV to +10 mV in 10 mV steps, followed by a test pulse of −10 mV during 80 ms were applied. (D) Dose-dependent inhibition curves of the Na^+ current by TTX. Currents were evoked at −20 mV from a holding potential of −120 mV during a pulse potential of 10 ms. The percentage of inhibition was calculated by comparing the current at a given concentration of toxin *versus* that obtained in its absence. Values represent the mean ± SEM of at least 6 independent experiments. (E) mRNA expression of $Na_v1.1$, $Na_v1.3$, and $Na_v1.6$ in the rat brain, but not in L6E9 cells. (F) $Na_v1.4$ and $Na_v1.5$ mRNA expression. RT-PCR reactions were set as described in the Materials and methods section with oligonucleotides described in SD Table 1. Rat skeletal muscle and heart were used as positive controls. PCR reactions were performed in the presence (+RT) and absence of the RT reaction (−RT). PCR products were run in a 2% agarose gel. (G) $Na_v1.4$ and $Na_v1.5$ mRNA expression levels quantified by real-time PCR. For each primer set, a standard curve was made and the slope factor calculated. The corresponding real-time PCR efficiency (E) of one cycle in the exponential phase was calculated according to the equation: $E = 10^{(-1/\text{slope})}$. The normalized $Na_v1.4$ and $Na_v1.5$ expression were calculated as follows: $((1+E)^{\Delta Ct(GOI)})/((1+E)^{\Delta Ct(control)})$, where Ct represents the threshold cycle; GOI, gene of interest; control, 18S. ***$p<0.001$ *vs.* $Na_v1.4$ (Student's t test). (H) Representative confocal images of Na_v1 immunofluorescence in L6E9 myoblasts. Left panel, DAPI staining of nuclei; Center panel, Na_v1 expression; Right panel, overlay of both images.

3. Results

3.1. Voltage-dependent $Na_v1.4$ and $Na_v1.5$ generate inward Na^+ currents in L6E9 myoblasts

Na^+ currents were evoked in L6E9 myoblasts (Fig. 1). Cells were held at −120 mV and 10 ms square pulses were applied from −90 to +60 mV in 10 mV steps (Fig. 1A). The threshold potential was ~−60 mV, and the I/V relationship exhibited a peak at −20 mV (Fig. 1B). Normalized conductance *versus* test potential indicated that the half-activation voltage was −36.8±2.2 mV with a k slope value of 7.4±0.4 mV (Fig. 1C). Steady-state availability curves were obtained by plotting current data *versus* test potential (Fig. 1C). The V_h was −80.9±2 mV with a slope factor of 6.6±0.2 mV. L6E9 cells expressed TTX-sensible and TTX-

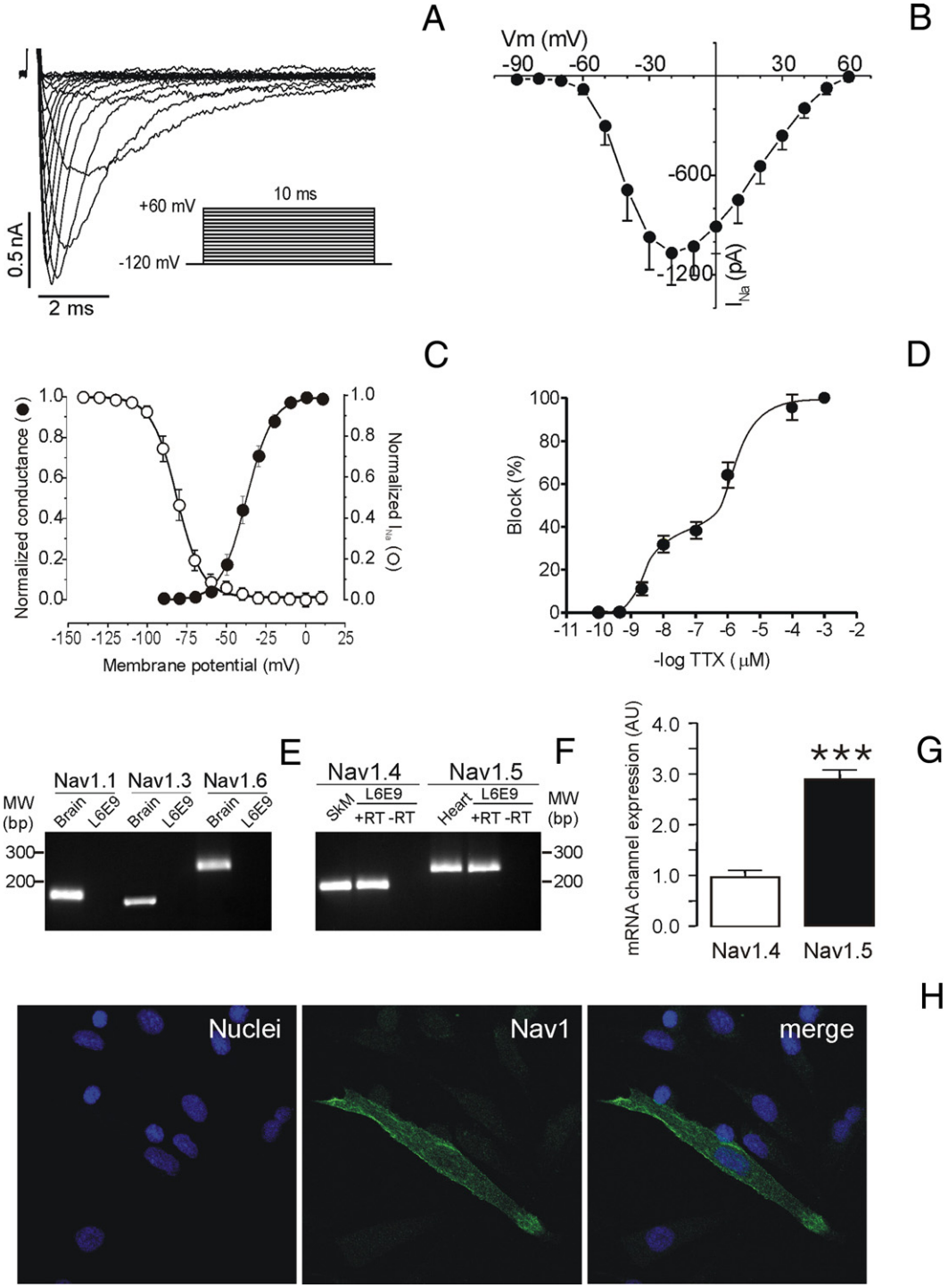

resistant channels (Fig. 1D). IC_{50} values were 0.8 nM and 1 μM for the high and the low-affinity, respectively. Na^+ currents evoked (−20 mV) in the presence of 100 nM TTX indicated that the TTX-sensitive current was about 40% of the total.

Several Na_v may be responsible for Na^+ currents in L6E9 [8]. $Na_v1.1$, $Na_v1.3$, $Na_v1.4$, $Na_v1.5$ and $Na_v1.6$ mRNA expression were analyzed, with only $Na_v1.4$ and $Na_v1.5$ being detected (Fig. 1E and F). Brain, heart and skeletal muscle were used as controls. $Na_v1.5$ expression was 3-fold that of $Na_v1.4$ (Fig. 1G). Five hundred μg of membrane protein was necessary to detect $Na_v1.5$ by Western blot (not shown). As such sample amounts render analysis difficult, we conducted immunodetection assays. Although several antibodies were used, the monoclonal anti-pan Na_v (Sigma, clone K58/35) yielded the best results (Fig. 1H).

3.2. Myoblast proliferation induces $Na_v1.4$ and $Na_v1.5$

Proliferation led to a 3-fold increase in Na^+ currents in L6E9 cells (Fig. 2A). Current intensity *versus* test potential plot indicated that currents shared voltage dependence (Fig. 2 B). V_h and k values of activation (Fig. 2C) and inactivation (Fig. 2D) were similar both in resting and proliferating cells. Half-activation voltages and slope values were −32.5±1.8 mV and 9.2±0.7 mV, and −36.8±2.2 mV and 8.3±0.3 mV for resting and proliferating myoblasts, respectively (SM Table 2). Similarly, V_h and the slope factor of the availability curves were −84.8±2.2 mV and 5.9±0.3 mV, and −81.2±2.1 mV and 6.4±0.3 mV in resting and proliferating cells, respectively (SM Table 2). Proliferation triggered a 3- to 4-fold transient increase in $Na_v1.4$ and $Na_v1.5$ mRNA expression (Fig. 2E) and the $Na_v1.5/Na_v1.4$ ratio remained constant (Fig. 2F). Since K^+ channels play a role during proliferation [17], we assessed whether Na_v channels would also be involved. Fig. 2G shows that TTX did not inhibit the proliferation-dependent ^{3}H-thymidine incorporation into myoblasts indicating that Na_v have no apparent role.

3.3. Myogenesis differentially regulates voltage-dependent Na^+ channels

SM Fig. 1 shows that myoblasts formed myotubes, with a fusion index over 60%. Concomitantly, while myogenin was early induced, MHC increased steadily. Na/K ATPase α1 subunit and β-actin controls remained constant [18].

Pulse potentials evoked Na^+ currents in 96 h-myotubes (Fig. 3A, SM Table 2). Currents were 4-fold higher in myotubes than in myoblasts and the peak current density steadily increased during myogenesis (Fig. 3B and C). The activation threshold shifted to −70 mV in myotubes (Fig. 3D). V_h shifted −11 mV (−48.2±3.4 *vs.* −36.8±2.2 mV) in myotubes (Fig. 3E) with no changes in the k slope (6.6±0.9 *vs.* 7.4±0.4 mV for myotubes and myoblasts, respectively). In addition, the half-inactivation voltage (Fig. 3F) was also more electronegative (−92.6±2.4 *vs.* −80.9±2.0 mV for myotubes and myoblasts, respectively). In order to differentiate between $Na_v1.4$ (TTX-sensible) and $Na_v1.5$ (TTX-resistant), currents were elicited in the presence of 100 nM TTX (Fig. 3G). While the contribution of TTX-sensitive component in myoblasts comprised about 40% of the total, this value decreased to 16% in myotubes (Fig. 3H).

$Na_v1.4$ and $Na_v1.5$ mRNA expression was analysed during myogenesis (Fig. 4A). Unlike $Na_v1.4$, $Na_v1.5$ increased steadily during differentiation and myotubes expressed much more $Na_v1.5$ (Fig. 4B). Myotubes expressed more Na_v protein (Fig. 4 F and K). Although the antibody recognized both $Na_v1.4$ and $Na_v1.5$, biophysical and pharmacological properties, and mRNA expression indicated that the increase in the Na_v signal stemmed from selective $Na_v1.5$ induction.

3.4. Myogenesis-induced $Na_v1.5$ efficiently targets to caveolae

Na_v target to caveolae in heart playing a mayor role in the cardiovascular system [19,20]. Myogenesis induced MHC and caveolin 3, as previously reported (Fig. 4C) [18,21]. However, caveolin 1 down-regulates during myogenesis [22]; thus, we used an anti-pan caveolin antibody. Fig. 4C shows that the overall caveolin abundance (cav1-3) remained constant. While Na_v weakly co-localized with caveolin in myoblasts (Fig. 4F–H), myogenesis-induced $Na_v1.5$ strongly co-localized with caveolin in myotubes (Fig. 4K–M).

3.5. $Na_v1.5$ plays a pivotal role during myogenesis

L6E9 cells were induced to differentiate in the presence of TTX. TTX (100 nM), which inhibits $Na_v1.4$, did not modify the expression of MHC and caveolin 3 (Fig. 5A and B). Surprisingly, in 2 out of 3 experiments, myogenin was induced. In contrast, 100 μM TTX, which blocks $Na_v1.5$, decreased MHC, caveolin 3, and myogenin. Again, the overall caveolin abundance did not change. In addition, 100 μM TTX generated fewer and smaller myotubes (Fig. 5C) and the fusion index was affected (Fig. 5D). While myotubes accounted for ~70% of the culture, 100 μM TTX reduced this value to <50%. Our results demonstrated that TTX, at doses which inhibited $Na_v1.5$, impaired the myogenesis of L6E9 myoblasts.

3.6. Neuregulin 1 further induced L6E9 myogenesis, concomitantly with an increase in $Na_v1.5$

Since myoblasts may be preconditioned prior to transplantation, we sought to determine whether NRGs, the growth factors involved in myocyte survival and differentiation [23,24], improved the cardiac-like phenotype. Cells were induced to differentiate and NRG (3 nM) was added 24 h later and studies were carried out after 2 days of NRG treatment [23]. NRG-treated cells achieved higher levels of

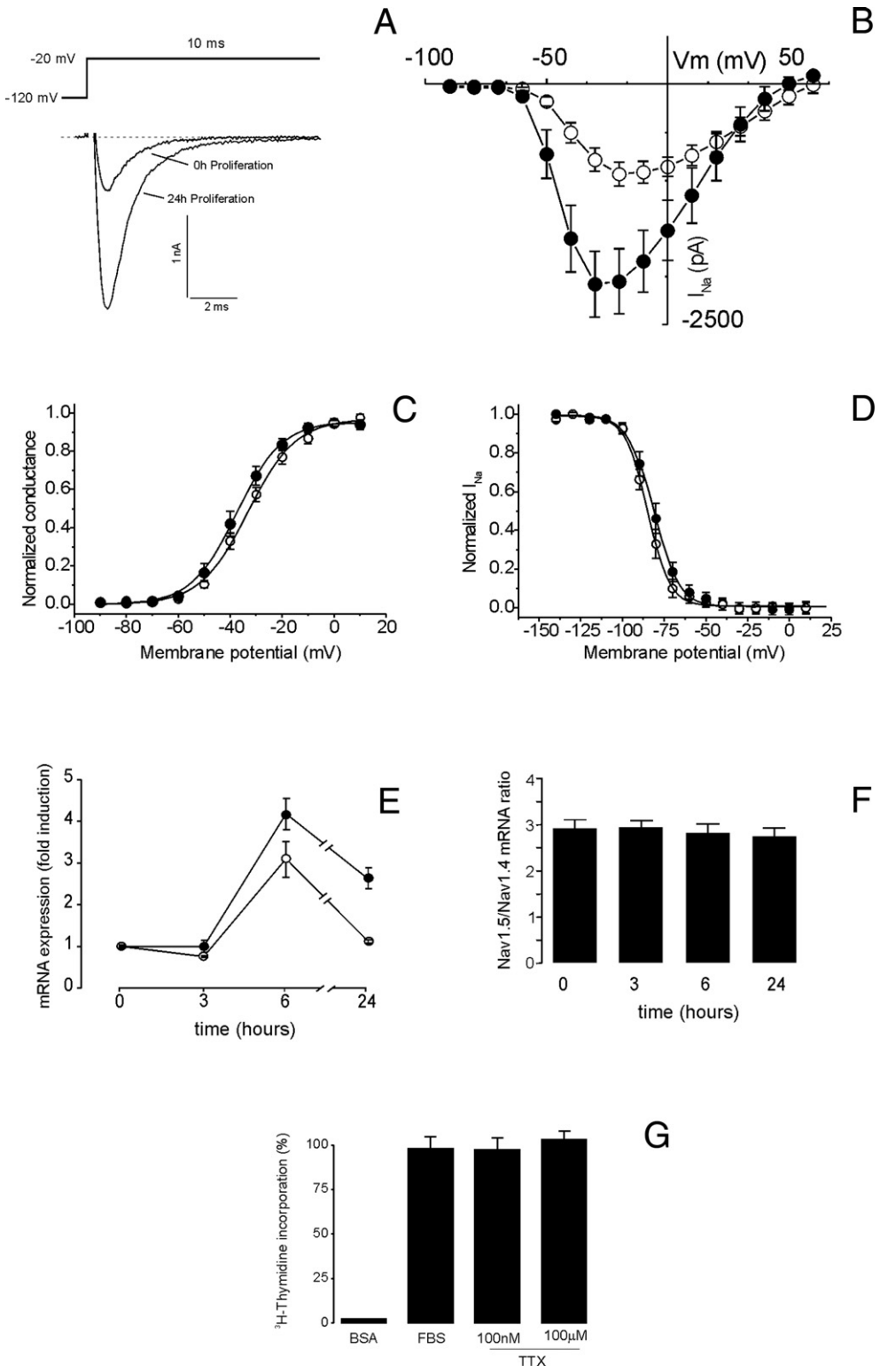

Fig. 2. Myoblast proliferation induced Na_v channels. (A) Representative traces of Na^+ currents. Resting cells were incubated for 24 h in the absence (resting) or presence of FBS (proliferation). Currents were elicited by a depolarizing step as indicated. (B) Current intensity *versus* voltage relationship of Na^+ currents. Cells were held at −120 mV and pulse potentials as described in Fig. 1 were applied. (C) Normalized conductance *versus* test potential plot. (D) Steady-state inactivation curves. A double-pulse protocol was applied as described in Fig. 1. Symbols for B–D are: ○, resting; ●, proliferation. (E) Proliferation induces $Na_v1.4$ and $Na_v1.5$ mRNA in L6E9 myoblasts. ○, $Na_v1.4$; ●, $Na_v1.5$. Samples were collected after the addition of FBS and real-time PCR analysis was performed at the indicated times. (F) $Na_v1.4/Na_v1.5$ mRNA ratio. The normalized $Na_v1.4$ and $Na_v1.5$ expression levels were calculated following the equation in Fig. 1. (G) TTX did not inhibit proliferation in L6E9 cells. Proliferating myoblasts were cultured in the presence of TTX (0.1 and 100 μM). Values represent the mean±SEM of 3 different assays, each done in triplicate.

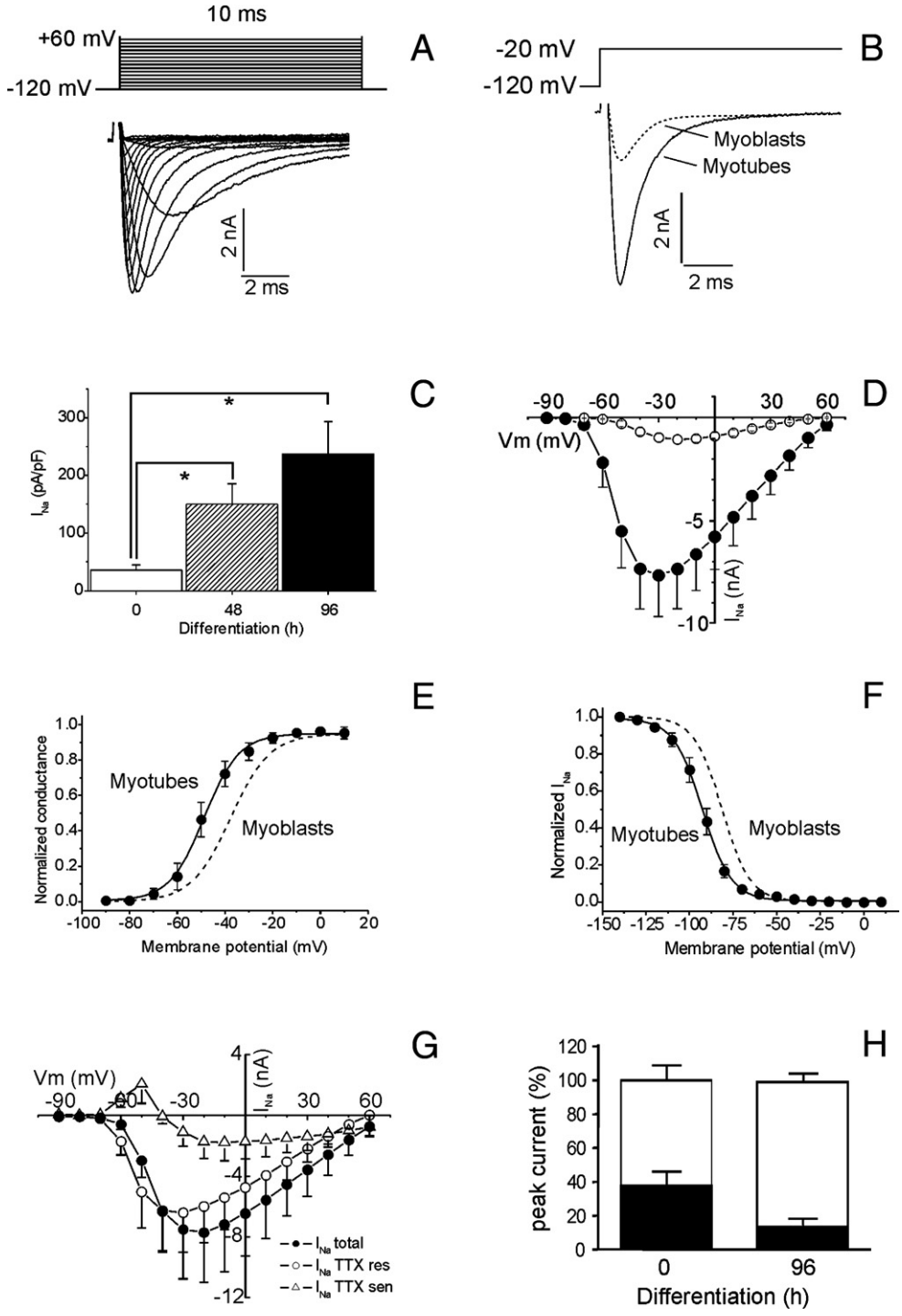

Fig. 3. Myogenesis induced Na_v currents. (A) Na^+ currents in myotubes. Currents were elicited in 96-h differentiated myotubes by depolarizing steps as indicated. (B) Representative traces of Na^+ currents in myoblasts and myotubes. (C) Current density plotted as a function of differentiation time. *$p < 0.05$ *vs.* 0 h, Student's *t* test. (D) Current intensity *versus* voltage relationship of Na^+ currents. Pulse potentials as described in panel A were applied. (E) Normalized conductance of Na^+ currents in myotubes *versus* test potential. (F) Steady-state inactivation curves. Dashed lines in B, E and F represent myoblasts. Symbols for D–F: ○, myoblasts; ●, myotubes. (G) Peak current plotted as a function of membrane potential in the presence of 100 nM TTX. The TTX-sensitive component was calculated by comparing the current at a given potential in the presence of the toxin *versus* that obtained in its absence. Symbols are: ●, overall intensity; ○, TTX-resistant; Δ, TTX-sensitive. (H) Major components of Na^+ currents in myoblasts (0 h) and myotubes (96 h). The peak current intensity (−20 mV) was considered 100%. TTX-sensitive and TTX-resistant components are calculated as shown in panel G. Open bars, TTX-resistant; closed bars, TTX-sensitive. Values represent the mean±SEM of at least 6 independent cells.

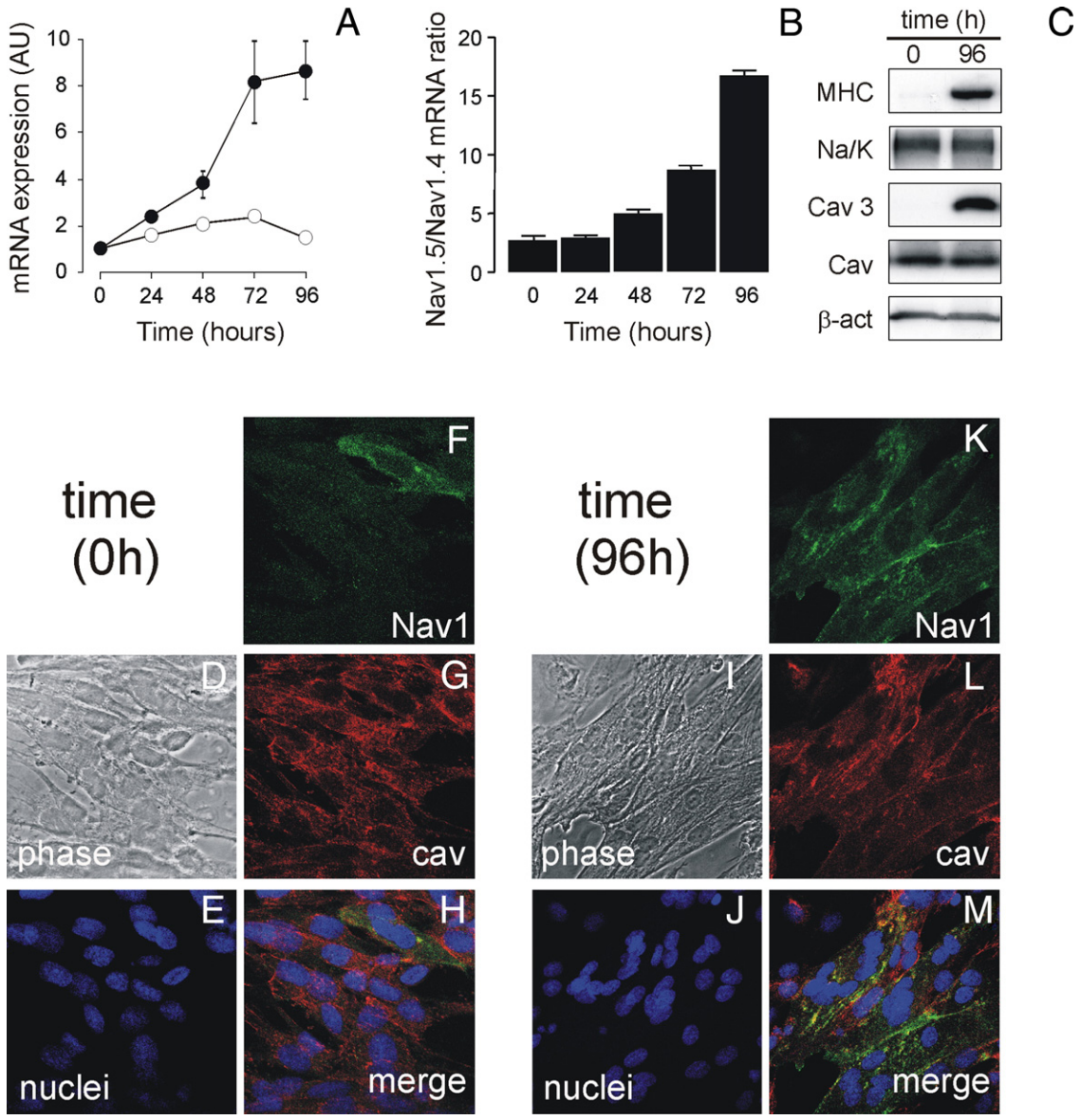

Fig. 4. Myogenesis specifically induces $Na_v1.5$ and co-localizes the channel with caveolin. (A) Real-time PCR was performed as described in Fig. 1. Differentiation was induced and samples were collected at the indicated times. Symbols are: ○, $Na_v1.4$; ●, $Na_v1.5$. (B) $Na_v1.4/Na_v1.5$ mRNA ratio. The normalized $Na_v1.4$ and $Na_v1.5$ expression levels were calculated following the equation in Fig. 1. Values represent the mean±SEM of 4 different assays, each done in triplicate. (C) Expression of myogenic markers. MHC, myosin heavy chain; Na/K, α_1 subunit of Na/K ATPase; Cav3, caveolin 3; Cav, overall caveolin (1–3); β-act, β-actin. (D-M) Immunofluorescence of Na_v1 and caveolin in L6E9 cells. (D–H) myoblasts (0 h). (I–M) myotubes (96 h). Na_v1, $Na_v1.X$; cav, overall caveolins; merge, overlay of signals.

differentiation, although 100 μM TTX inhibited myogenesis (Fig. 6A and B). In addition, NRG further increased $Na_v1.5$ expression but had no effect on $Na_v1.4$ (Fig. 6C). Moreover, we further confirmed the role of $Na_v1.5$ (Fig. 6D). TTX diminished NRG-induced MHC and caveolin 3 expression. NRG did not alter the myogenin expression, indicating that its induction occurred before the addition of NRG (Fig. 6D). These results were further confirmed by immunofluorescence of caveolin 3 (SM Fig. 2). Caveolin 3 immunoreactivity increased in the presence of NRG while TTX diminished the signal.

3.7. Differential expression of $Na_v1.4$ and $Na_v1.5$ during proliferation and differentiation in human skeletal muscle cells

To further confirm the data of L6E9 cells, we performed a serial of experiments in primary human skeletal muscle cultures (SM Fig. 3). Human myoblasts were induced to proliferate during 24 h and to differentiate for 5 days. MHC expression increased in myotubes (SM Fig. 3A). While proliferation induced $Na_v1.4$ and $Na_v1.5$, differentiation specifically increased $Na_v1.5$ (SM Fig. 3B–D). Unlike neonatal L6E9 cells, $Na_v1.4$ mRNA was much more abundant

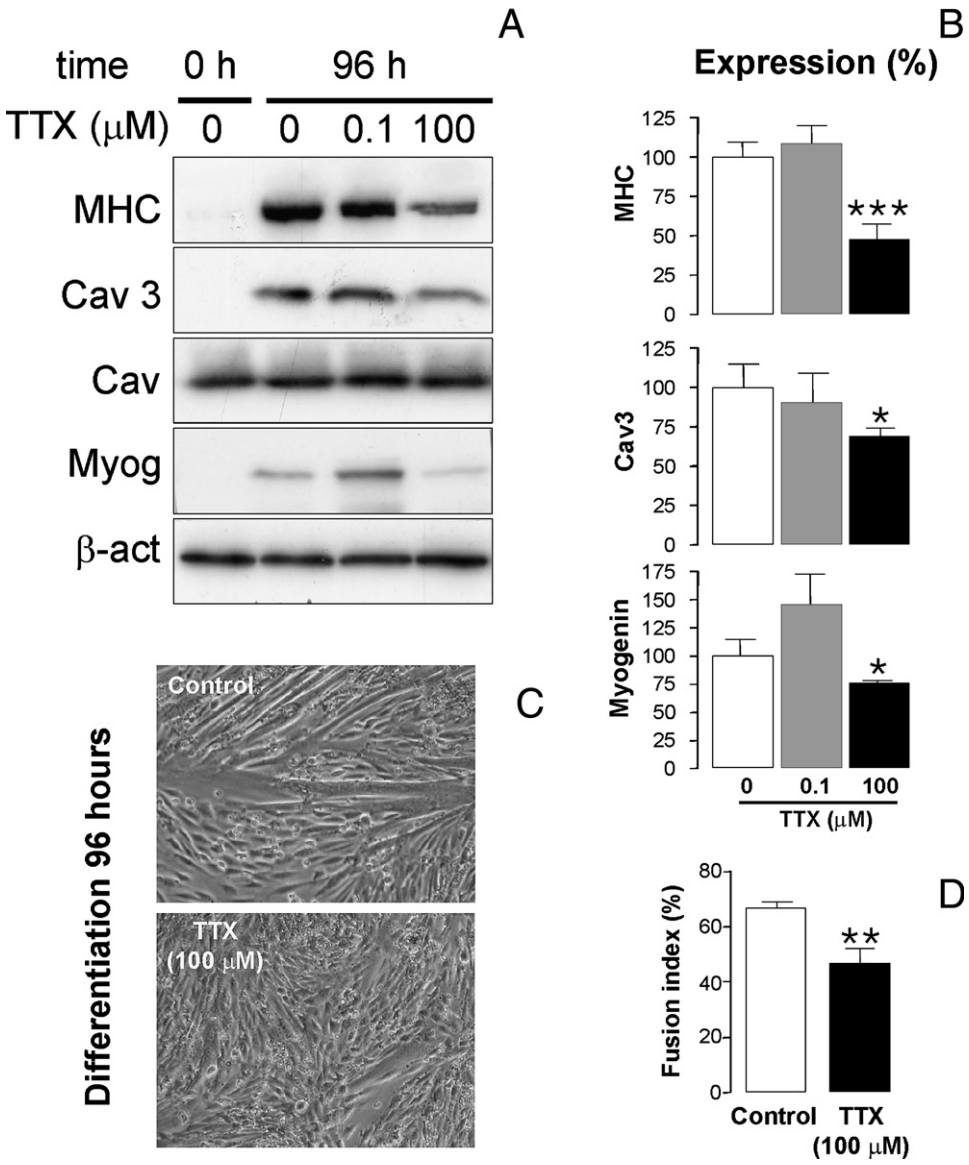

Fig. 5. $Na_v1.5$ is involved in myogenesis. (A) Protein expression of myogenic markers was impaired by the presence of TTX. MHC, myosin heavy chain; Cav3, caveolin 3; Cav, overall caveolin (cav1-3); Myog, myogenin; β-act, β-actin. (B) Percentage of expression. At least 4 Western blots were performed and the relative abundances of MHC, Cav3 and Myogenin were analyzed. (C) Phase images of differentiated L6E9 in the absence or presence of 100 μM TTX. (D) Fusion index in the absence or presence of 100 μM TTX. Open bars, no TTX; grey bars, 0.1 μM TTX; closed bars, 100 μM TTX. Values represent the mean± SEM of at least 4 independent experiments. *$p<0.05$; **$p<0.01$; ***$p<0.001$ *vs.* control (0 TTX), Student's *t* test.

than $Na_v1.5$ in adult human myoblasts (SM Fig. 3C and D). While the $Na_v1.4$/ $Na_v1.5$ ratio ($\Delta Ct_{(Nav1.5-Nav1.4)}$) remained constant during proliferation, myogenesis triggered an important decrease (SM Fig. 3C and D). However, $Na_v1.4$ was still predominant in adult skeletal myotubes as previously described [12]. Furthermore, immunocytochemistry further confirmed the $Na_v1.5$ accumulation in myotubes (SM Fig. 3E).

4. Discussion

The use of skeletal myoblasts for cardiac repair in patients with myocardial infarction has been an active field of research in recent years [1–4]. Skeletal myoblasts form contractile myofibers and the acquisition of a cardiac phenotype is crucial to successful engraftment. The expression of cardiac proteins, such as ion channels, is important for the establishment of electromechanical junctions. Therefore, an understanding of the molecular events underlying engraftment is essential to improving this cellular therapy.

Since Na_v are the main proteins involved in the propagation of cardiac action potential [6,7], we analyzed the physiological regulation of Na_v during proliferation and myogenesis in skeletal myoblasts. The neonatal skeletal muscle cell line L6E9 expresses $Na_v1.4$ and $Na_v1.5$. Unlike C2C12 cell line, the cardiac-like $Na_v1.5$ expression was strong in L6E9 myoblasts [14]. L6E9 cells do not contract *in*

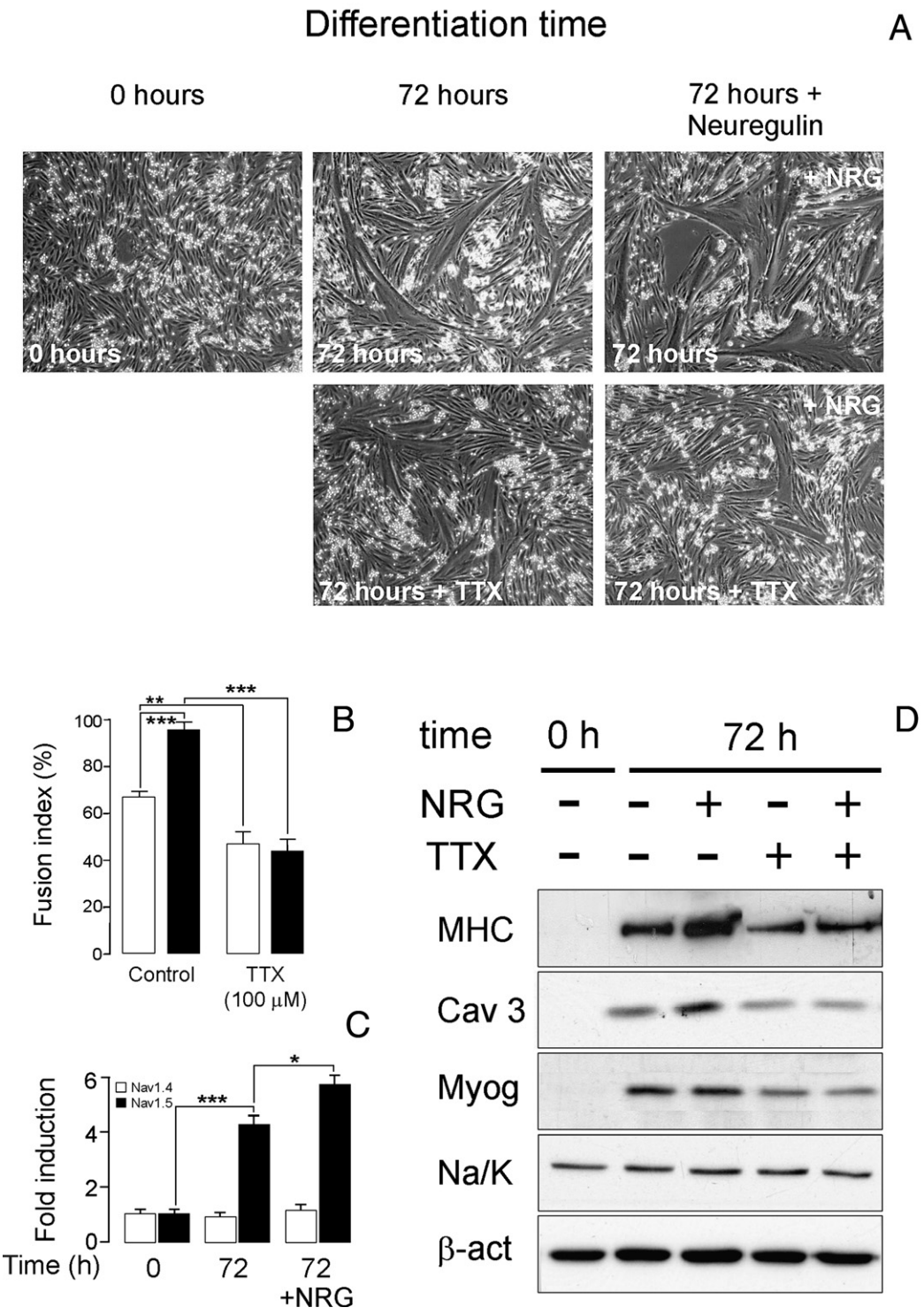

Fig. 6. Neuregulin-dependent myogenesis further induced $Na_v1.5$ in L6E9 cells. Myoblasts were induced to differentiate by serum depletion in the presence or absence of 100 μM TTX. NRG was added (+NRG) 24 h after the cells were changed to the low serum medium, and studies were carried out after 2 days of NRG treatment (72 h of differentiation). (A) Phase images of L6E9 cells. (B) Fusion index of L6E9 cells in the presence (closed bars) or absence (open bars) of NRG, (C) $Na_v1.4$ (open bars) and $Na_v1.5$ (closed bars) mRNA expression. Values represent the mean±SEM of at least 3 independent experiments. *$p<0.05$; **$p<0.01$; ***$p<0.001$ (Student's t test). (D) Expression of myogenic markers. Protein extracts were analyzed by Western blot. MHC, myosin heavy chain; Cav 3, caveolin 3; Myog, myogenin; Na/K, α_1 subunit of Na/K ATPase; β-act, β-actin.

vitro, suggesting an early state of differentiation [25]. This is relevant to our results. Mature skeletal muscle expresses Na^+ channels that are sensitive to TTX [12], which is in agreement with our human skeletal muscle cell cultures. However, embryonic muscles synthesize TTX-insensitive isoforms [8,12]. In this context, myoblasts preconditioned in culture express more TTX-resistant cardiac-like Na_v. Differentiated C2C12 myotubes express a low Na_v-cardiac phenotype but $Na_v1.5$ slightly increases (~30%) and electrophysiological parameters shift to more hyperpolarised values in conditioned cardiac culture media [14]. However, L6E9 myotubes augmented more than 8 fold $Na_v1.5$ and this was further increased by the presence of NRG. Our data indicate that by using weakly differentiated skeletal myoblasts (i.e., foetal or neonatal), cells achieved higher levels of the cardiac phenotype.

Unlike cardiomyocytes, skeletal myocytes proliferate. We describe, for the first time, Na_v expression during skeletal myocyte proliferation. We found a mRNA increase concomitantly with a raise in Na^+ conductance. This could be a consequence of changes in the membrane potential during the cell cycle progression, in which K^+ channels are involved [17]. However, unlike K^+ channels, Na^+ channels do not play any apparent role.

TTX-resistant Na^+ channels account for over 90% of Na^+ currents in adult cardiac myocytes. The remaining 10% are generated by neural $Na_v1.X$, skeletal muscle $Na_v1.4$, and probably other Na_vX [5,11]. This is similar to what we found in myotubes. Na^+ currents in L6E9 myoblasts have V_h around −35 mV, which is higher than the value of $Na_v1.4$ (−25 mV), but lower than that of $Na_v1.5$ (−40 mV). Previous works demonstrate that C2C12 cells only achieved a Na_v-like current phenotype (−43 mV) by culturing myotubes in conditioned cardiac culture media [14]. However, L6E9 myotubes expressed Na^+ channels that were half maximally open at a membrane potential around −48 mV, quite similar to $Na_v1.5$ [9,10]. Comparable analyses reflected similar inactivation rates, whereby cardiac $Na_v1.5$ and L6E9 myotubes share more hyperpolarised values [9].

Localization of ion channels is also necessary for proper electrical signalling [19,20]. While cardiac-Na_v target to caveolin-rich domains [19], their localization in skeletal muscle remained unknown. Myogenic-induced $Na_v1.5$ co-localized with caveolin, which places the channels in close proximity to signalling molecules. Thus, the β-adrenergic receptor stimulation of cardiac sodium channels is associated with caveolae in the sarcolemma, a localization which improves cardiac performance [19].

Unlike proliferation, $Na_v1.5$ is involved in myogenesis, in which K^+ channels play a pivotal role [18,26–28]. Na_v are responsible for the initiation and propagation of action potentials [6,7]. Therefore, changes in membrane potential may be preceded by Na_v functions. Low concentrations of TTX induce myogenin and Na_v currents [29,30]. In this scenario, myogenin promotes myogenesis [29,31]. Our data in no way challenge this result. TTX (100 nM) did not inhibit myogenesis, but rather increased myogenin ~50%. However, higher doses of TTX decreased differentiation.

Cardiomyoplasty with cells expressing distinct electrophysiological properties may cause side effects [1–4]. Thus, preconditioning myoblasts appears to improve cardiac phenotype acquisition [14,15]. However, the percentage of cells that survive and differentiate following transplantation remains very low [3]. We found that NRG, a survival factor involved in cardiomyocyte and skeletal myocyte differentiation [23,24], further induced the Na_v cardiac-phenotype *in vitro*. Alternative approaches, such as intramyocardial injection in conjunction with coronary artery bypass or combined cardiomyoplasty with bone marrow cells, increases the graft survival [4,32]. Coronary artery bypass and revascularization with bone marrow cells improve ischemic area perfusion and cardiac function [3,32,33]. In this context, our NRG results have physiological relevance. Similar to what occurs in coronary bypasses, NRG increases glucose uptake [23]. In addition, NRG stimulates the survival of neurons surrounding cortical brain injuries *in vivo* [34].

Cardiomyoplasty is not only feasible, but has been associated with improved cardiac function. While the Myoblast Autologous Grafting in Ischemic Cardiomyography (MAGIC) trial failed to reach its main objectives, the experience partially reversed remodeling indicating that additional experimental studies are still warranted in order to address important issues central to improving this cellular therapy. Therefore, knowledge of the molecular events surrounding myoblast engraftment is crucial.

Acknowledgements

Supported by the Ministerio de Educación y Ciencia (MEC), Spain (BFI2002-00764 and BFU2005-00695 to AF; SAF2005-00489 to AG; SAF2004-06856, CAM GR/SAL/0854/2004 and FIS RD06/0014/0006 to CV). RMM, RS and NV hold fellowships from the MEC and MRF from the Generalitat de Catalunya. We thank the editorial assistance of the Language Advisory Service (University of Barcelona). RMM and MD contributed equally. CV and AF contributed equally.

Appendix A. Supplementary data

Supplementary data associated with this article can befound, in the onlineversion, at doi:10.1016/j.cardiores.2007.08.009.

References

[1] Hagege AA, Marolleau JP, Vilquin JT, Alheritiere A, Peyrard S, Duboc D, et al. Skeletal myoblast transplantation in ischemic heart failure: long-term follow-up of the first phase I cohort of patients. Circulation 2006;114:I108–13.
[2] Murry CE, Field LJ, Menasche P. Cell-based cardiac repair: reflections at the 10-year point. Circulation 2005;112:3174–83.
[3] van den Bos EJ, Davis BH, Taylor DA. Transplantation of skeletal myoblasts for cardiac repair. J Heart Lung Transplant 2004;23:1217–27.
[4] Memon IA, Sawa Y, Miyagawa S, Taketani S, Matsuda H. Combined autologous cellular cardiomyoplasty with skeletal myoblasts and bone

marrow cells in canine hearts for ischemic cardiomyopathy. J Thorac Cardiovasc Surg 2005;130:646–53.
[5] Haufe V, Camacho JA, Dumaine R, Gunther B, Bollensdorff C, von Banchet GS, et al. Expression pattern of neuronal and skeletal muscle voltage-gated Na+ channels in the developing mouse heart. J Physiol 2005;564:683–96.
[6] Yu FH, Catterall WA. Overview of the voltage-gated sodium channel family. Genome Biol 2003;4:207.
[7] Hodgkin AL, Huxley AF, Katz B. Measurement of current-voltage relations in the membrane of the giant axon of Loligo. J Physiol 1952;116:424–48.
[8] Catterall WA, Goldin AL, Waxman SG. International Union of Pharmacology. XLVII. Nomenclature and structure-function relationships of voltage-gated sodium channels. Pharmacol Rev 2005;57:397–409.
[9] Wang DW, George Jr AL, Bennett PB. Comparison of heterologously expressed human cardiac and skeletal muscle sodium channels. Biophys J 1996;70:238–45.
[10] Bennett ES. Channel activation voltage alone is directly altered in an isoform-specific manner by Na(v1.4) and Na(v1.5) cytoplasmic linkers. J Membr Biol 2004;197:155–68.
[11] Felipe A, Knittle TJ, Doyle KL, Tamkun MM. Primary structure and differential expression during development and pregnancy of a novel voltage-gated sodium channel in the mouse. J Biol Chem 1994;269:30125–31.
[12] Yang JS, Sladky JT, Kallen RG, Barchi RL. TTX-sensitive and TTX-insensitive sodium channel mRNA transcripts are independently regulated in adult skeletal muscle after denervation. Neuron 1991;7:421–7.
[13] Frelin C, Vijverberg HP, Romey G, Vigne P, Lazdunski M. Different functional states of tetrodotoxin sensitive and tetrodotoxin resistant Na+ channels occur during the in vitro development of rat skeletal muscle. Pflugers Arch 1984;402:121–8.
[14] Zebedin E, Mille M, Speiser M, Zarrabi T, Sandtner W, Latzenhofer B, et al. C2C12 skeletal muscle cells adopt cardiac-like sodium current properties in a cardiac cell environment. Am J Physiol Heart Circ Physiol 2007;292:H439–50.
[15] Muthuchamy M, Pajak L, Wieczorek DF. Induction of endogenous myosin light chain 1 and cardiac alpha-actin expression in L6E9 cells by MyoD1. J Biol Chem 1992;267:18728–34.
[16] de Luna N, Gallardo E, Soriano M, Dominguez-Perles R, de la Torre C, Rojas-Garcia R, et al. Absence of dysferlin alters myogenin expression and delays human muscle differentiation “in vitro”. J Biol Chem 2006;281:17092–8.
[17] Felipe A, Vicente R, Villalonga N, Roura-Ferrer M, Martinez-Marmol R, Sole L, et al. Potassium channels: new targets in cancer therapy. Cancer Detect Prev 2006;30:375–85.
[18] Grande M, Suarez E, Vicente R, Canto C, Coma M, Tamkun MM, et al. Voltage-dependent K+ channel beta subunits in muscle: differential regulation during postnatal development and myogenesis. J Cell Physiol 2003;195:187–93.
[19] Yarbrough TL, Lu T, Lee HC, Shibata EF. Localization of cardiac sodium channels in caveolin-rich membrane domains: regulation of sodium current amplitude. Circ Res 2002;90:443–9.
[20] O’Connell KM, Martens JR, Tamkun MM. Localization of ion channels to lipid Raft domains within the cardiovascular system. Trends Cardiovasc Med 2004;14:37–42.
[21] Carrasco M, Canicio J, Palacin M, Zorzano A, Kaliman P. Identification of intracellular signaling pathways that induce myotonic dystrophy protein kinase expression during myogenesis. Endocrinology 2002;143:3017–25.
[22] Parton RG, Way M, Zorzi N, Stang E. Caveolin-3 associates with developing T-tubules during muscle differentiation. J Cell Biol 1997;136:137–54.
[23] Suarez E, Bach D, Cadefau J, Palacin M, Zorzano A, Guma A. A novel role of neuregulin in skeletal muscle. Neuregulin stimulates glucose uptake, glucose transporter translocation, and transporter expression in muscle cells. J Biol Chem 2001;276:18257–64.
[24] Giraud MN, Fluck M, Zuppinger C, Suter TM. Expressional reprogramming of survival pathways in rat cardiocytes by neuregulin-1beta. J Appl Physiol 2005;99:313–22.
[25] Kubo Y. Comparison of initial stages of muscle differentiation in rat and mouse myoblastic and mouse mesodermal stem cell lines. J Physiol 1991;442:743–59.
[26] Fischer-Lougheed J, Liu JH, Espinos E, Mordasini D, Bader CR, Belin D, et al. Human myoblast fusion requires expression of functional inward rectifier Kir2.1 channels. J Cell Biol 2001;153:677–86.
[27] Bernheim L, Bader CR. Human myoblast differentiation: Ca(2+) channels are activated by K(+) channels. News Physiol Sci 2002;17:22–6.
[28] Occhiodoro T, Bernheim L, Liu JH, Bijlenga P, Sinnreich M, Bader CR, et al. Cloning of a human ether-a-go-go potassium channel expressed in myoblasts at the onset of fusion. FEBS Lett 1998;434:177–82.
[29] Ugarte G, Brandan E. Transforming growth factor beta (TGF-beta) signaling is regulated by electrical activity in skeletal muscle cells. TGF-beta type I receptor is transcriptionally regulated by myotube excitability. J Biol Chem 2006;281:18473–81.
[30] Sherman SJ, Catterall WA. Electrical activity and cytosolic calcium regulate levels of tetrodotoxin-sensitive sodium channels in cultured rat muscle cells. Proc Natl Acad Sci U S A 1984;81:262–6.
[31] Konig S, Hinard V, Arnaudeau S, Holzer N, Potter G, Bader CR, et al. Membrane hyperpolarization triggers myogenin and myocyte enhancer factor-2 expression during human myoblast differentiation. J Biol Chem 2004;279:28187–96.
[32] Herreros J, Prosper F, Perez A, Gavira JJ, Garcia-Velloso MJ, Barba J, et al. Autologous intramyocardial injection of cultured skeletal muscle-derived stem cells in patients with non-acute myocardial infarction. Eur Heart J 2003;24:2012–20.
[33] Haider H, Ashraf M. Bone marrow stem cell transplantation for cardiac repair. Am J Physiol Heart Circ Physiol 2005;288:H2557–67.
[34] Tokita Y, Keino H, Matsui F, Aono S, Ishiguro H, Higashiyama S, et al. Regulation of neuregulin expression in the injured rat brain and cultured astrocytes. J Neurosci 2001;21:1257–64.